Proteasome Function Is Required for DNA Damage Response and Fanconi Anemia Pathway Activation

Céline Jacquemont and Toshiyasu Taniguchi

Divisions of Human Biology and Public Health Sciences, Fred Hutchinson Cancer Research Center, Seattle, Washington

Abstract

Proteasome inhibitors sensitize tumor cells to DNA-damaging agents, including ionizing radiation (IR), and DNA cross-linking agents (melphalan and cisplatin) through unknown mechanisms. The Fanconi anemia pathway is a DNA damage–activated signaling pathway, which regulates cellular resistance to DNA cross-linking agents. Monoubiquitination and nuclear foci formation of FANCD2 are critical steps of the Fanconi anemia pathway. Here, we show that proteasome function is required for the activation of the Fanconi anemia pathway and for DNA damage signaling. Proteasome inhibitors (bortezomib and MG132) and depletion of 19S and 20S proteasome subunits (PSMD4, PSMD14, and PSMB3) inhibited monoubiquitination and/or nuclear foci formation of FANCD2, whereas depletion of DSS1/SHFM1, a subunit of the 19S proteasome that also directly binds to BRCA2, did not inhibit FANCD2 monoubiquitination or foci formation. On the other hand, DNA damage–signaling processes, such as IR-induced foci formation of phosphorylated ATM (phospho-ATM), 53BP1, NBS1, BRCA1, FANCD2, and RAD51, were delayed in the presence of proteasome inhibitors, whereas ATM autophosphorylation and nuclear foci formation of γH2AX, MDC1, and RPA were not inhibited. Furthermore, persistence of DNA damage and abrogation of the IR-induced G_1-S checkpoint resulted from proteasome inhibition. In summary, we showed that the proteasome function is required for monoubiquitination of FANCD2, foci formation of 53BP1, phospho-ATM, NBS1, BRCA1, FANCD2, and RAD51. The dependence of specific DNA damage–signaling steps on the proteasome may explain the sensitization of tumor cells to DNA-damaging chemotherapeutic agents by proteasome inhibitors. [Cancer Res 2007;67(15):7395–405]

Introduction

The ubiquitin-proteasome system is responsible for the vast majority of protein degradation in eukaryotes (1). The 26S proteasome (constituted of the catalytic 20S proteasome and the regulatory 19S proteasome) controls the destruction of damaged and abnormally folded proteins as well as protein turnover, hence tightly regulating multiple cellular processes. Ubiquitin is a reversible and versatile regulatory signal, which controls degradation of proteins through Lys^{48} polyubiquitination but also modifies the subcellular localization and catalytic activity of proteins through monoubiquitination and Lys^{63} polyubiquitination (2). Ubiquitin dynamic is ensured by activating (E1) and conjugating (E2) enzymes and ubiquitin ligases (E3) required for its covalent binding to the target proteins and by deubiquitinating enzymes catalyzing its removal and recycling.

Proteasome inhibitors are natural [β-lactones (lactacystin), epipolythioldioxopiperazine, etc.] and synthetic products {peptide aldehyde [MG132, MG115, *N*-acetyl-Leu-Leu-Nle-CHO (ALLN), and PSI], peptide boronates (bortezomib), etc.}, which mostly inhibit the chymotryptic-like activity of the 20S proteasome (β5 subunit), although β1 and β2 subunits may also be inhibited *in vivo* by bortezomib (3). Proteasome inhibitors show antitumor activities through proapoptotic and antiproliferative mechanisms (4). Bortezomib has recently been approved for treatment of multiple myeloma and mantle cell lymphoma and is currently being tested for treatment of other malignancies (5).

Proteasome inhibitors also sensitize tumor cells to widely used cancer therapeutics, including ionizing radiation (IR; ref. 6), and DNA cross-linking agents (melphalan and cisplatin; refs. 7, 8). They sensitize myeloma cells to melphalan and doxorubicin (7) and ovarian cancer cells to cisplatin (8). Clinical trials show promising results for combination of bortezomib with melphalan and other drugs in myeloma treatment (9) and with carboplatin (a cisplatin derivative) in ovarian cancer treatment (10). However, the molecular bases of the sensitization to DNA-damaging agents by proteasome inhibitors remain unclear.

The Fanconi anemia pathway (Supplementary Fig. S1*A*) is a DNA damage–activated signaling pathway critical for cellular resistance to DNA interstrand cross-links (reviewed in ref. 11). Inherited biallelic mutations in 1 of the 13 known Fanconi anemia genes cause Fanconi anemia, a rare genetic cancer-prone disorder characterized by cellular hypersensitivity to DNA cross-linking agents. Eight Fanconi anemia proteins assemble in the Fanconi anemia core complex, which is required for FANCD2 monoubiquitination during normal S phase, and, together with ATR and RPA, in response to exogenous DNA damage (12–14). Fanconi anemia core complex is considered to be the ubiquitin ligase (E3), and UBE2T the E2, for FANCD2 monoubiquitination (15, 16). Monoubiquitinated FANCD2 is targeted, in a BRCA1-dependent manner, to nuclear foci where it colocalizes with DNA damage signaling and repair proteins, including BRCA1, RAD51, and BRCA2/FANCD1 (12). FANCD2 monoubiquitination and nuclear foci formation are critical for the function of the Fanconi anemia pathway, and lack of these steps causes cellular hypersensitivity to DNA cross-linking agents (12). A deubiquitinating enzyme, USP1, deubiquitinates monoubiquitinated FANCD2 and negatively regulates the Fanconi anemia pathway (17). Importantly, the integrity of the Fanconi anemia pathway is required for tumor resistance to cisplatin (reviewed in ref. 11). Consequently, drugs inhibiting the Fanconi anemia pathway may sensitize tumor cells to DNA cross-linking agents.

In response to DNA lesions, cells initiate cascades of phosphorylation/recruitment events, mostly mediated by the ATM and ATR

Note: Supplementary data for this article are available at Cancer Research Online (http://cancerres.aacrjournals.org/).

Requests for reprints: Toshiyasu Taniguchi, Divisions of Human Biology and Public Health Sciences, Fred Hutchinson Cancer Research Center, 1100 Fairview Avenue North, C1-015, Seattle, WA 98109-1024. Phone: 206-667-7283; Fax: 206-667-5815; E-mail: ttaniguc@fhcrc.org.

doi:10.1158/0008-5472.CAN-07-1015

kinases. Activation of the Fanconi anemia pathway is one of those numerous cellular responses to DNA damage.

The proteasome has been implicated in DNA repair in yeast. Sem1/DSS1/SHFM1 protein is a newly identified subunit of the 19S proteasome in both yeast and human cells (18). In yeast, Sem1 is recruited with the 19S and 20S proteasomes to DNA double-strand breaks (DSB) *in vivo* and is required for efficient repair of DSB by homologous recombination (HR) and nonhomologous end-joining pathways (18). Human DSS1/SHFM1 physically binds to BRCA2/FANCD1 and is required for its stability and function (19–21) and, consequently, for efficient formation of RAD51 nucleofilaments required for HR. However, the involvement of the proteasome in DNA repair in mammalian cells has not been shown yet.

We hypothesized that inhibition of the DNA damage response in general, and in particular inhibition of the Fanconi anemia pathway, may be involved in the chemosensitization to DNA-damaging agents by proteasome inhibitors. We found that proteasome inhibitors inhibit both monoubiquitination and nuclear foci formation of FANCD2 as well as DNA damage–signaling processes, such as foci formation of phosphorylated ATM (phospho-ATM), 53BP1, NBS1, BRCA1, and RAD51. The inhibition of both the Fanconi anemia pathway and DNA damage response may explain the sensitization of tumor cells to DNA-damaging agents induced by proteasome inhibitors.

Materials and Methods

Cell lines and culture conditions. HeLa, IMR90, and TOV21G (FANCF-inactivated ovarian cancer cells) were purchased from the American Type Culture Collections. FANCF-corrected TOV21G cells (TOV21G+FANCF) were described previously (22). GFPu-1 cells (23) were a gift of Dr. Muneesh Tewari (Fred Hutchinson Cancer Research Center, Seattle, WA). Cell lines were grown in DMEM supplemented with 10% FCS. γ-Irradiation was delivered using a linear accelerator. For UV-C (254 nm) irradiation, cells were washed in PBS and irradiated in the absence of liquid using a 2400 UV Stratalinker (Stratagene). For cisplatin, hydroxyurea (Sigma), MG132, ALLN (Calbiochem), lactacystin (Biomol International), and bortezomib (Millennium Pharmaceuticals) treatments, cells were continuously exposed to the drug for the indicated time. Cells used for Western blotting, RNA extraction, immunofluorescence, and cell cycle analyses were generally issued from one single culture dish.

Small interfering RNA transfection. Expression of targeted genes was knocked down by transient transfection of small interfering RNA (siRNA) directed against DSS1 (5′-AAGGTAGACTTAGGTCTGTTA-3′), PSMB3 (Hs_PSMB3_6_HP Validated siRNA, Qiagen), PSMD4 (5′-AAGGAGGAAGACAAGAAGTGA-3′), PSMD14 (5′-TAGGACATGAACCAAGACAAA-3′), UCH37 (5′-ACCGAGCTCATTAAAGGATTC-3′), USP1 (5′-TCGGCAATACTTGCTATCTTA-3′; ref. 17), and USP14 (5′-AGCATCGTAACACCAGAAGAT-3′; Qiagen). Negative controls were obtained by transfection of nontargeting siRNA (5′-AATTCTCCGAACGTGTCACGT-3′). Cells (2×10^5) were transfected with siRNA oligos (final concentration, 50 nmol/L) using HiPerFect reagent (Qiagen). Cells were analyzed 48 h after transfection of siRNA targeting proteasome subunits and 72 to 96 h after transfection of USP1 siRNA. Efficiency of siRNA treatment was evaluated by semiquantitative reverse transcription-PCR (RT-PCR) and/or Western blotting. Total RNAs were extracted using Trizol reagent (Invitrogen), and 1 μg RNA was used for reverse transcription reaction using SuperScript III (Invitrogen) and oligo(dT) primers. PCR was done using following PCR primers: DSS1-L, TTCCCCAAGTCTCTATGGTAGC; DSS1-R, TAGTGTCCCATCCTGGGTTC; PSMB3-L, CCGGTTTACTGGAATTGCTC; PSMB3-R, CTGGGAACAGGGTTAGTCCA; PSMD4-L, ACCGGTTCTCATCTGGTGAC; PSMD4-R, GCTACCCTTTCCCTCCAGTC; PSMD14-L, GGGCAACTCTTTTGAATGGA; PSMD14-R, GCCTTCCTGTCTGCTTCAAC; USP14-L, GTTGGAGCTTGGCTGAAGAC; USP14-R, GTCAAGGGTCCTGGAACAAA; UCH37-L, GGATGTCCATTTAGGCGAGA; UCH37-R, CCTGAGCTTTCTTTGCGTTC; ACTB-L, AAGAGAGGCATCCTCACCCT; and ACTB-R, GGAAGGAAGGCTGGAAG. Images of agarose gels were acquired using ChemiDoc XRS apparatus and QuantiOne software (Bio-Rad). ImageJ software was used for densitometry quantification.

Western blot analysis. Whole-cell extracts were obtained by direct lysis of cells in lysis buffer [0.05 mol/L Tris-HCl (pH 6.8), 2% SDS, 6% β-mercaptoethanol] boiled for 5 min. SDS-PAGE electrophoresis was done using NuPAGE 3% to 8% Tris-acetate or NuPAGE 4% to 12% Tris-glycine gels (Invitrogen), and proteins were transferred on nitrocellulose membranes using a submerged transfer apparatus. Mouse monoclonal antibodies directed against FANCD2 (FI-17, 1:200 dilution; Santa Cruz Biotechnology), γH2AX (#05-636, 1:1,000; Upstate), proliferating cell nuclear antigen (PCNA; PC10, 1:1,000; Santa Cruz Biotechnology), PSMB3 (PW8130, 1:1,000; Biomol International), PSMD4 (PW9250, 1:1,000; Biomol International), USP14 (H00009097-M04, 1:2,000; Novus Biologicals), and rabbit polyclonal antibodies against USP1 [C-term, 1:3,000; gift of Drs. Tony Huang (New York University School of Medicine, New York, NY) and Alan D'Andrea (Dana Farber Cancer Institute, Boston, MA); ref. 24] were used as primary antibodies. Horseradish peroxidase–conjugated enhanced chemiluminescence anti-mouse and anti-rabbit IgG (1:5,000; Amersham) were used as secondary antibodies. Chemiluminescence was used for detection (Perkin-Elmer Life Sciences). Films were digitalized using a standard scanner and images were processed using Photoshop CS (Adobe Systems, Inc.). ImageJ software was used for densitometry quantification.

Immunofluorescence microscopy. Cells were grown on coverslips in tissue culture plates and treated as indicated with DNA-damaging agents and proteasome inhibitors. Coverslips were fixed with 2% paraformaldehyde in PBS for 20 min, permeabilized with 0.5% Triton X-100 in PBS for 10 min, and incubated in blocking buffer (PBS + 5% bovine serum albumin + 0.1% Tween 20) for 30 min. Specific primary antibodies diluted in blocking buffer were incubated for 2 h at room temperature or overnight at 4°C. Mouse monoclonal antibodies detecting ATM-Ser1981P (#200-301-400, 1:1,000; Rockland), BRCA1 (D-9, 1:100; Santa Cruz Biotechnology), γH2AX (JBW301, 1:1,000; Upstate), and RPA2 (NA18, 1:300; Calbiochem) and rabbit polyclonal antibodies detecting FANCD2 (NB 100-182, 1:1,000; Novus Biologicals), MDC1 (1:1,000; gift of Dr. Junjie Chen, Yale University, New Haven, CT), NBS1 (NB 100-143, 1:200; Novus Biologicals), RAD51 (PC130, 1:1,000; Calbiochem), and 53BP1 (PC712, 1:500; Calbiochem) were used as primary antibodies. Species-specific fluorescein- or Cy3-conjugated secondary antibodies (Jackson ImmunoResearch) diluted in blocking buffer (1:1,000) were incubated for 1 h at room temperature. Nuclei were counterstained with 4′,6-diamidino-2-phenylindole (1 μg/mL). Coverslips were mounted on slides in Vectashield (Vector Laboratories). Two-dimensional acquisitions were made with a microscope (TE2000, Nikon) equipped with a 40× immersion objective (1.3 numerical aperture) and a CCD camera (CoolSNAP ES, Photometrics). Images were acquired and analyzed using MetaVue (Universal Imaging). At least 100 cells per experimental point were scored for presence of foci, and each experiment was repeated at least thrice independently.

Flow cytometry analyses. Exponentially growing cells were plated in drug-free medium 24 h before experiment and then exposed to DNA-damaging agents and proteasome inhibitors as described. For cell cycle analyses, cells were pulse labeled with 30 μmol/L 5-bromo-2′-deoxyuridine (BrdUrd; Sigma) for 15 min, washed twice with PBS, and fixed with 70% ice-cold ethanol. Cells were then stained for DNA content (propidium iodide) and BrdUrd incorporation with anti-BrdUrd rat monoclonal antibody (MAS250, Harlan Sera-Lab) followed by FITC-conjugated goat anti-rat antibody (Jackson ImmunoResearch). For analyses of green fluorescent protein (GFP) expression in GFPu-1 cells, control and proteasome inhibitor–treated and siRNA-treated live cells resuspended in ice-cold PBS were analyzed. 1×10^5 cells were analyzed for each experimental point. Fluorescence data were plotted using CellQuest software (Becton Dickinson) and FlowJo (Tree Star, Inc.). Three independent experiments were carried out for each condition.

Results

Proteasome inhibitors inhibited monoubiquitination and nuclear foci formation of FANCD2. First, we investigated the

effect of proteasome inhibitors on FANCD2 monoubiquitination and nuclear foci formation (Fig. 1). FANCD2 monoubiquitination was significantly increased by cellular exposure to cisplatin (Fig. 1*A*, compare *lane 6* with *lane 1*). An additional 8-h incubation with proteasome inhibitors (MG132, bortezomib, lactacystin, and ALLN) induced a decrease of both basal and cisplatin-induced FANCD2 monoubiquitination (Fig. 1*A, lanes 2–5* and *7–10*). FANCD2 monoubiquitination is required for its targeting into nuclear foci at sites of DNA damage (12). Consistently, proteasome inhibitors inhibited cisplatin-induced nuclear foci formation of FANCD2 (Fig. 1*A, bottom*), whereas γH2AX foci formation was not inhibited. Similar results were observed in IMR90 human primary fibroblasts and a FANCF-corrected TOV21G ovarian cancer cell line (TOV21G+FANCF; data not shown). Bortezomib (or MG132; data not shown) inhibited monoubiquitination of FANCD2 induced by various DNA-damaging agents (IR, cisplatin, hydroxyurea, and UV irradiation) in HeLa (Fig. 1*B*), IMR90, and TOV21G+FANCF cells (data not shown). IR-induced monoubiquitination and foci formation of FANCD2 were dramatically inhibited by proteasome inhibitors for up to 12 h in HeLa and IMR90 (Fig. 1*C*) as well as in TOV21G+FANCF cells (data not shown).

Changes in the proportion of S-phase cells may affect FANCD2 monoubiquitination and foci formation (13). Hydroxyurea treatment, which blocks cells in early S phase, induced monoubiquitination of FANCD2 (Fig. 1*D*). Treatment with proteasome inhibitors for up to 8 h did not significantly alter the cell cycle distribution and proportion of cells in S phase (nor increased apoptosis; data not shown) in both asynchronous and hydroxyurea-treated HeLa cells (Fig. 1*D, bottom*), whereas basal and hydroxyurea-induced FANCD2 monoubiquitination were inhibited (Fig. 1*D, top*).

In summary, proteasome inhibitors strongly inhibited both basal and DNA damage–induced FANCD2 monoubiquitination and foci formation in various cell types through a mechanism independent of cell cycle deregulation.

Proteasome is required for the activation of the Fanconi anemia pathway. To confirm the role of proteasome in Fanconi anemia pathway activation, we knocked down the expression of several proteasome subunits (Fig. 2*A*): PSMB3 (β3), a structural subunit of the 20S proteasome; PSMD4 (Rpn10), the polyubiquitin receptor of the 19S proteasome; DSS1/SHFM1, part of the 19S proteasome, which also directly binds to BRCA2/FANCD1; PSMD14 (Rpn11) and UCH37, both deubiquitinating enzymes part of the 19S proteasome; and USP14, another deubiquitinating enzyme associated with the 19S proteasome.

Efficiency of the depletions is presented in Fig. 2*A* and their effect on proteasome catalytic function (measured using GFPu-1 cells expressing GFP coupled to a short degron, which allows to monitor proteasome activity through GFP expression; ref. 23) in Fig. 2*B*. Depletion of PSMD14 severely decreased proteasome proteolytic activity and led to a significant inhibition of FANCD2 monoubiquitination (Fig. 2*C*, compare *lanes 16–18* with *lanes 13–15*) and foci formation (Fig. 2*D*) in HeLa cells. PSMB3 and PSMD4 depletion slightly decreased proteasome activity and inhibited FANCD2 foci formation (Fig. 2*D*), whereas inhibition of FANCD2 monoubiquitination was minimal (Fig. 2*C, lanes 1–9*). DSS1, USP14, and UCH37 depletion minimally affected proteasome activity (Fig. 2*B*). DSS1 and UCH37 knockdown did not inhibit FANCD2 monoubiquitination or foci formation (Fig. 2*C, lanes 10–12* and *22–24*, and *D*). Surprisingly, depletion of USP14 significantly inhibited FANCD2 foci formation (Fig. 2*D*) but did not inhibit FANCD2 monoubiquitination (Fig. 2*C, lanes 19–21*). These results confirm the requirement of proteasome proteolytic function for the activation of the Fanconi anemia pathway and show that inhibition of FANCD2 monoubiquitination requires a more profound proteasome inhibition than inhibition of FANCD2 foci formation, suggesting that the proteasome affects these two events independently. These data also suggest a specific role for USP14 in FANCD2 foci formation.

Specific inhibition of FANCD2 monoubiquitination by proteasome inhibition. To test whether proteasome inhibition affects monoubiquitination processes in general, we compared the effect of proteasome inhibitors on FANCD2 and PCNA monoubiquitination. Both FANCD2 and PCNA are nuclear proteins monoubiquitinated in response to DNA damage and colocalize at sites of DNA damage on chromatin. They also share the same deubiquitinating enzyme USP1 (17, 24, 25), which is the only known deubiquitinating enzyme for FANCD2 and PCNA.

FANCD2, but not PCNA, monoubiquitination was inhibited by MG132 in cells treated with cisplatin, IR, hydroxyurea, and UV (Fig. 3*A*). Treatment of mock- and hydroxyurea-treated HeLa cells with increasing concentrations of MG132 revealed a dose-dependent inhibition of FANCD2 monoubiquitination and a reciprocal up-regulation of PCNA monoubiquitination (Fig. 3*B*). These results show that proteasome inhibitor–induced inhibition of monoubiquitination is specific to FANCD2. Proteasome inhibition can lead to the depletion of cellular free ubiquitin (26), but the increase of hydroxyurea-induced PCNA monoubiquitination in the presence of increasing doses of proteasome inhibitor (Fig. 3*B, lanes 11* and *12*) suggests that cellular free ubiquitin is still available to modify nuclear proteins.

Expression of USP1 protein, the unique known deubiquitinating enzyme for FANCD2 and PCNA, was not increased, but rather decreased, in the presence of proteasome inhibitor (Fig. 3*C*), indicating that FANCD2 deubiquitination is not due to USP1 stabilization induced by proteasome inhibition. Even after USP1 knockdown, which efficiency was shown by the increased spontaneous FANCD2 and PCNA monoubiquitination (Fig. 3*D, lane 7* compared with *lane 1*), the addition of MG132 led to a rapid decrease of both spontaneous and hydroxyurea-induced FANCD2 monoubiquitination (Fig. 3*D, lanes 7–12*), suggesting the involvement of other deubiquitinating enzyme(s). Among the three deubiquitinating enzymes associated with the proteasome (PSMD14, USP14, and UCH37), USP14 is activated on treatment with proteasome inhibitor *in vivo* (27) and has been reported to interact with FANCC (28), therefore seemed as a good candidate for proteasome inhibitor–activated deubiquitinating enzyme for FANCD2. However, depletion of these deubiquitinating enzymes (USP14, UCH37, and PSMD14) failed to reverse proteasome inhibition–induced deubiquitination of FANCD2 (Fig. 2*B, lanes 18, 21*, and *24*), indicating that they are not responsible for the proteasome inhibitor–induced deubiquitination of FANCD2. The responsible deubiquitinating enzyme remains unknown.

FANCD2 monoubiquitination is dependent on Fanconi anemia core complex (E3), UBE2T (E2), and ATR (Supplementary Fig. S1*A*; refs. 12, 14, 16). Treatment with MG132 did not decrease the expression of the components of the Fanconi anemia core complex (FANCA, FANCC, FANCE, FANCF, FANCG, and FANCM) or UBE2T and did not affect coimmunoprecipitation of FANCC with FANCA, revealing the formation of the Fanconi anemia core complex (Supplementary Fig. S1*B–D*). In the conditions we used (2 μmol/L MG132 for 12 h), no stabilization of FANCC was observed, although it has been reported after longer exposure to higher dose of MG132 (29). ATR is required for monoubiquitination of FANCD2 in

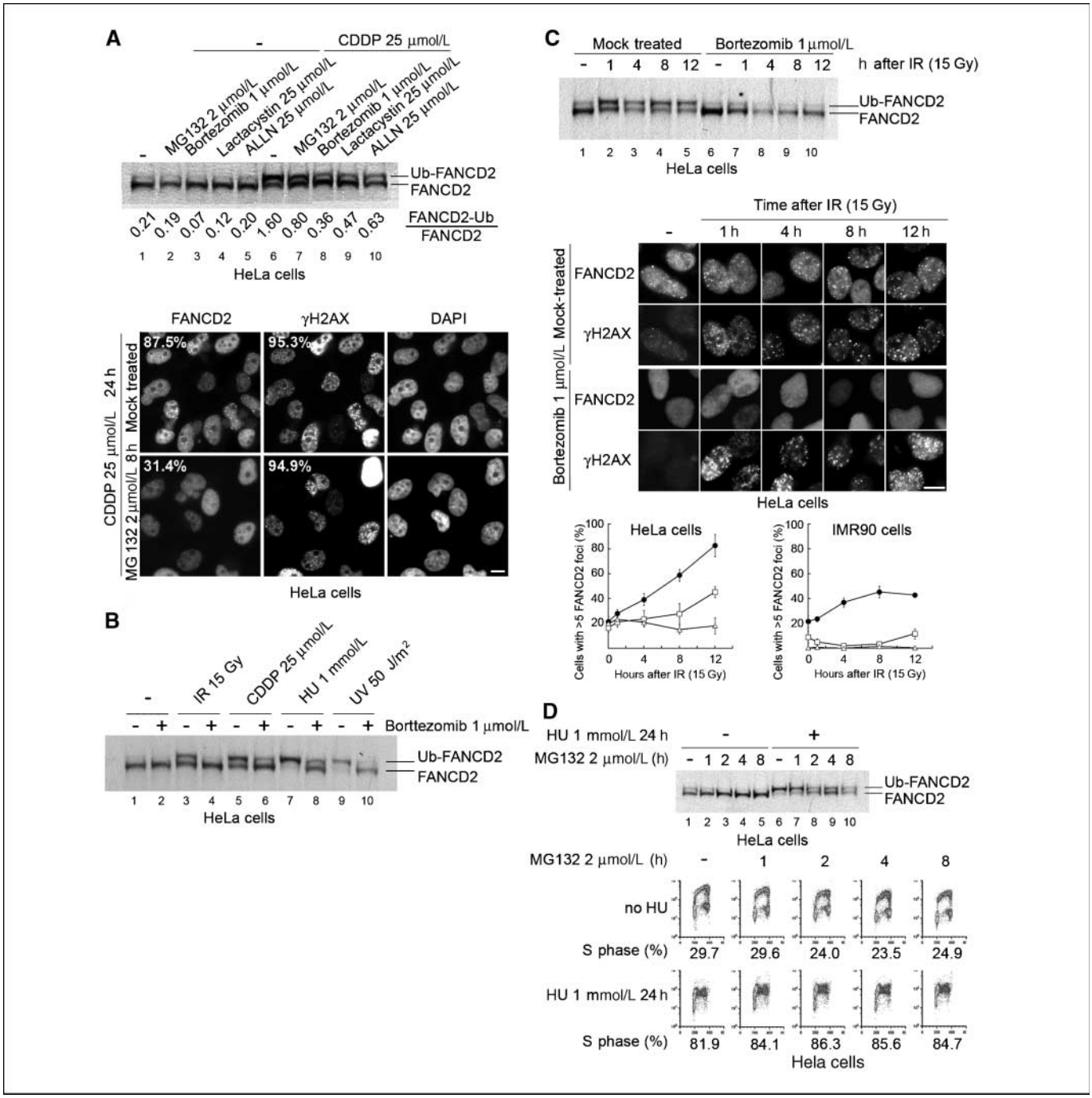

Figure 1. Proteasome inhibitors inhibit the Fanconi anemia pathway. (Full-length blots are presented in Supplementary Fig. S3*A–D*). *A,* proteasome inhibitors inhibited cisplatin-induced FANCD2 monoubiquitination and foci formation. HeLa cells were mock treated or incubated in the presence of cisplatin (*CDDP*; 25 μmol/L) for 24 h and then with proteasome inhibitors at the indicated concentration for the following 8 h. Whole-cell extracts were subjected to FANCD2 immunoblotting. Ratios (FANCD2-Ub/FANCD2) are indicated for each condition. Representative pictures of cells immunostained with FANCD2 and γH2AX antibodies are shown with the percentage of cells harboring at least five FANCD2 or γH2AX foci. *DAPI,* 4′,6-diamidino-2-phenylindole. *Bar,* 20 μm. *B,* FANCD2 monoubiquitination induced by different DNA-damaging agents was inhibited by proteasome inhibition. HeLa cells were incubated with cisplatin (25 μmol/L) or hydroxyurea (*HU*; 1 mmol/L) for 24 h or subjected to IR (15 Gy) or UV irradiation (50 J/m^2) and incubated with bortezomib (1 μmol/L) for 8 h immediately after cisplatin removal, during the last 8 h of hydroxyurea treatment, or immediately after IR and UV irradiation, respectively. *C,* proteasome inhibitors inhibited IR-induced FANCD2 monoubiquitination and foci formation for up to 12 h after generation of DNA damage. HeLa cells and IMR90 primary human fibroblasts were pretreated with bortezomib (1 μmol/L) or MG132 (2 μmol/L) for 4 h, irradiated (15 Gy), and incubated in the presence of the corresponding proteasome inhibitor for the indicated duration. Whole-cell extracts from HeLa cells were subjected to FANCD2 immunoblotting, and cells were immunostained for FANCD2 and γH2AX. Representative pictures of mock- and bortezomib-treated HeLa cells are shown, together with the proportion of HeLa and IMR90 cells with at least five FANCD2 foci as a function of the time after exposure to IR in mock-treated (●), MG132-treated (□), or bortezomib-treated (Δ) populations. *Points,* mean; *bars,* SE. *Bar,* 20 μm. *D,* proteasome inhibition did not affect cell cycle distribution of mock- and hydroxyurea-treated HeLa cells, whereas basal and hydroxyurea-induced FANCD2 monoubiquitination was strongly affected. HeLa cells were mock treated or incubated with hydroxyurea (1 mmol/L) for 24 h, and MG132 (2 μmol/L) was added at the indicated time before the end of hydroxyurea treatment. Whole-cell extracts were subjected to FANCD2 immunoblotting. Cells were pulse labeled with BrdUrd (30 μmol/L) for 15 min at the end of the 24-h treatment with hydroxyurea. Incorporation of BrdUrd (*Y axis*) and DNA content (propidium iodide; *X axis*) was quantified by flow cytometry. Representative flow cytometric analyses and the mean value of the proportion of cells in S phase are shown for each condition.

response to exogenous DNA damage but not for basal FANCD2 monoubiquitination (14), whereas proteasome inhibitors inhibited both basal and DNA damage–induced monoubiquitination of FANCD2. ATR-dependent CHK1 phosphorylation on Ser^{345} induced by cisplatin, hydroxyurea, and UV (30) was not inhibited by proteasome inhibitors (Supplementary Fig. S2*A*), whereas CHK1 phosphorylation after IR was inhibited (Supplementary Fig. S2*B*). These results argue against a general role of ATR inhibition

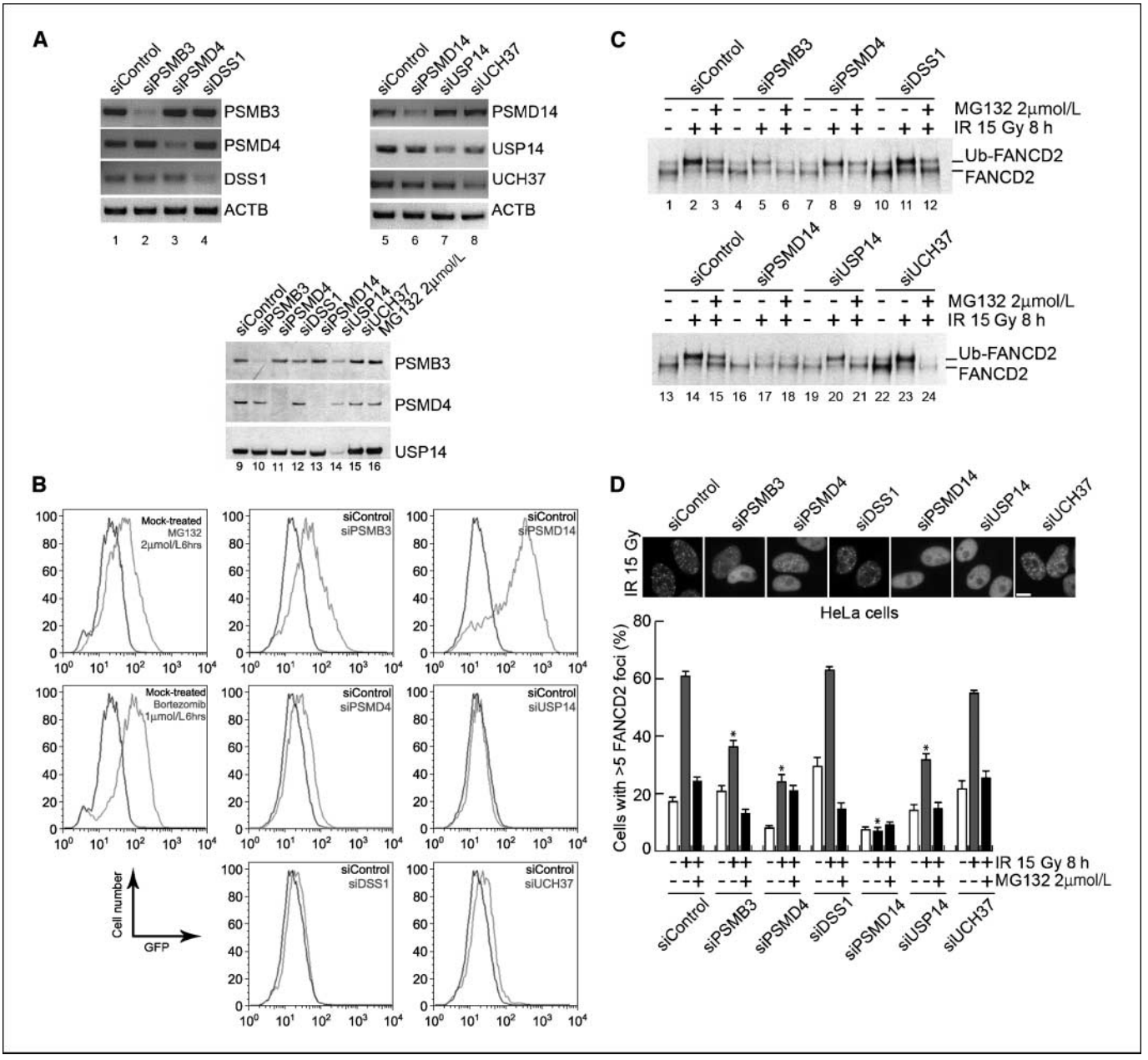

Figure 2. Depletion of proteasome subunits inhibits the activation of the Fanconi anemia pathway. (Full-length blots/gels are presented in Supplementary Fig. S3*E* and *F*). *A,* efficiency of proteasome subunit depletion. *Lanes 1* to *8,* semiquantitative RT-PCR analysis of mRNA expression in PSMB3-, PSMD4-, DSS1-, PSMD14-, USP14-, and UCH37-depleted cells 48 h after siRNA transfection (depletion efficiency was 75% for PSMB3, 65% for PSMD4, 44% for DSS1, 63% for PSMD14, 45% for USP14, and 43% for UCH37); *lanes 9* to *16,* whole-cellular extracts were also subjected to PSMB3, PSMD4, and USP14 immunoblots (depletion efficiency was 86% for PSMB3, 99% for PSMD4, and 79% for USP14). PSMD14 depletion led to a concomitant down-regulation of PSMD4 protein expression probably due to the destabilization of the 19S proteasome induced by the lack of PSMD14 protein. *B,* depletion of PSMD14 strongly inhibited proteasome function, whereas depletion of PSMB3 and PSMD4 had a mild effect and depletion of USP14, UCH37, and DSS1 had only a minor effect on proteasome function. GFPu-1 cells expressing GFP fused to a short degron were used to assess proteasome proteolytic function. Forty-eight hours after siRNA transfection, as well as 6 h after treatment with MG132 (2 μmol/L) and bortezomib (1 μmol/L), cells were harvested, washed in PBS, and analyzed by flow cytometry for GFP expression. Representative flow cytometry histograms. The experiments were independently repeated thrice with consistent results. *C,* IR-induced FANCD2 monoubiquitination was strongly inhibited by PSMD14 depletion, minimally affected by PSMB3, PSMD4, DSS1, USP14, and UCH37 depletion. Forty hours after siRNA transfection, HeLa cells were irradiated and treated with/without MG132 for 8 h after IR. Whole-cell extracts were subjected to FANCD2 immunoblotting. *D,* depletion of PSMB3, PSMD4, PSMD14, and USP14, but not DSS1 and UCH37, led to inhibition of IR-induced FANCD2 foci formation. Cells were treated as in (*B*). Representative pictures of cells immunostained with anti-FANCD2 antibody. Percentage of cells harboring at least five FANCD2 foci before (*white columns*), 8 h after IR (*gray columns*), and 8 h after IR in the presence of MG132 (*black columns*). *Bars,* SE. *, significant difference with irradiated control siRNA–transfected cells ($P < 0.05$, unpaired *t* test). *Bar,* 20 μm.

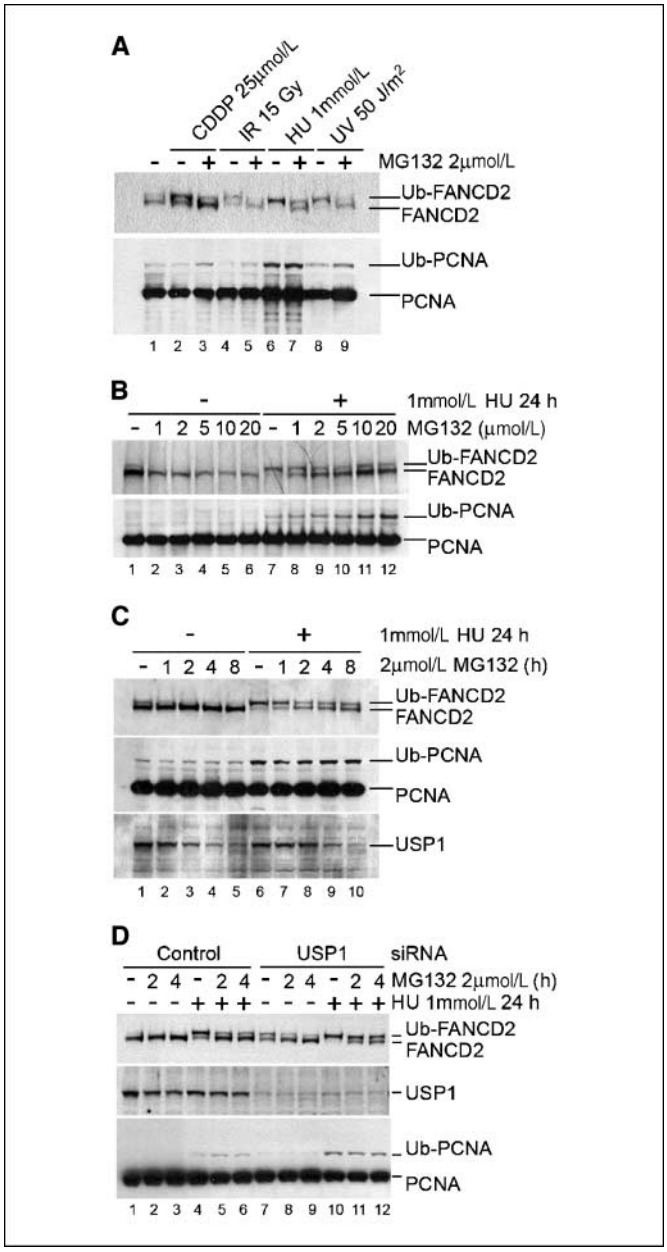

Figure 3. Proteasome inhibitors inhibit FANCD2 monoubiquitination but not PCNA monoubiquitination. (Full-length blots are presented in Supplementary Fig. S3*G–J*). *A,* proteasome inhibitors inhibited DNA damage–induced FANCD2 monoubiquitination but did not inhibit PCNA monoubiquitination. HeLa cells were mock treated or incubated with cisplatin (25 μmol/L) or hydroxyurea (1 mmol/L) for 24 h or subjected to IR (15 Gy) or UV irradiation (50 J/m^2) and incubated with MG132 (2 μmol/L) for 8 h immediately after cisplatin removal, during the last 8 h of hydroxyurea treatment, or immediately after IR and UV irradiation, respectively. Whole-cell extracts were subjected to FANCD2 and PCNA immunoblotting. *B,* inhibition of FANCD2 monoubiquitination and reciprocal up-regulation of PCNA monoubiquitination increased with the dose of proteasome inhibitors. Increasing doses of MG132 (0–20 μmol/L) were applied for 8 h to mock- and hydroxyurea-treated HeLa cells. Whole-cell extracts were subjected to FANCD2 and PCNA immunoblotting. *C,* USP1 expression decreased in the presence of proteasome inhibitors. HeLa cells were mock treated or incubated with hydroxyurea (1 mmol/L) for 24 h, and MG132 was added at the indicated time before the end of hydroxyurea treatment. Whole-cell extracts were subjected to FANCD2, PCNA, and USP1 immunoblotting. *D,* knockdown of USP1 expression did not impede the inhibition of FANCD2 monoubiquitination induced by proteasome inhibitors. Seventy-two hours after indicated siRNA transfection, cells were exposed to hydroxyurea (1 mmol/L) for 24 h, and MG132 was added at the indicated time before the end of hydroxyurea treatment. Whole-cell extracts were subjected to FANCD2, PCNA, and USP1 immunoblotting.

in the proteasome inhibition–induced inhibition of FANCD2 monoubiquitination, although it may be involved specifically after IR treatment. Taken together, proteasome inhibition leads to the specific inhibition of FANCD2 monoubiquitination by mechanisms other than USP1 activation, ATR inhibition, and decreased expression of the Fanconi anemia core complex (E3) and UBE2T (E2).

Proteasome inhibitors inhibit IR-induced DNA damage response. Next, we systematically tested which steps of the IR-induced DNA damage response are inhibited by proteasome inhibitors. Proteasome inhibitors did not inhibit the detection and early signaling of DNA damage, as IR-induced foci formation of γH2AX, MDC1, and RPA was not inhibited in MG132- or bortezomib-treated HeLa and IMR90 primary fibroblasts (Fig. 4). In contrast, bortezomib and MG132 delayed foci formation of phospho-ATM (Ser^{1981}), 53BP1, NBS1, and BRCA1 and strongly inhibited RAD51 (Fig. 4) and FANCD2 (Fig. 1*C*) foci formation up to 12 h after exposure to IR. Knockdown of proteasome subunits (PSMB3, PSMD4, and PSMD14) and USP14 led to an impaired IR-induced foci formation of BRCA1, RAD51 (Fig. 5), and FANCD2 (Fig. 2*D*). Consistently, cisplatin-induced foci formation of FANCD2 (Fig. 1*A*), phospho-ATM, BRCA1, and RAD51, but not γH2AX and RPA, was inhibited by proteasome inhibitors and by depletion of proteasome subunits (data not shown).

DNA damage signaling is propagated by multiple phosphorylation events catalyzed by protein kinases, such as ATM, ATR, CHK2, and CHK1. As IR-induced phospho-ATM foci formation was inhibited by proteasome inhibitors, we evaluated the status of ATM autophosphorylation (Ser^{1981}) and IR-induced ATM-dependent phosphorylation of NBS1 (Ser^{343}), CHK2 (Thr^{68}), and FANCD2 (Thr^{691}; refs. 31–34) on proteasome inhibition (Supplementary Fig. S2*C*). None of these phosphorylation events was affected by proteasome inhibition, suggesting that ATM activation is not inhibited by proteasome inhibitors. In contrast, IR-induced CHK1 phosphorylation was inhibited (Supplementary Fig. S2*B*), suggesting that IR-induced activation of ATR is inhibited by proteasome inhibition. In addition, RPA phosphorylation induced by all the DNA-damaging agents tested (IR, UV, cisplatin, and hydroxyurea) seemed to be inhibited by proteasome inhibition (Supplementary Fig. S2*B*). Current data indicate that RPA phosphorylation, which is dependent on ATM, ATR, and DNA-PKcs, down-regulates DNA replication and participates in intra-S-phase checkpoint but does not affect DNA repair (35).

DSS1 depletion inhibited RAD51 foci formation, as reported previously (20, 21), but not FANCD2 or BRCA1 foci formation, and minimally affected proteolytic function of the proteasome (Figs. 2*B* and *D* and 5). These results suggest that, in human cells, DSS1 is critical for RAD51 foci formation but plays only a minor role in the proteolytic function of the proteasome. The discrepancy with the requirement of Sem1/DSS1 in yeast for proteolytic function of the proteasome (36) may be related to the existence of the BRCA2 protein in vertebrates to which DSS1 directly binds.

Our results suggest a particular role for the proteasome-linked deubiquitinating enzyme USP14 in the activation of DNA damage response independently of proteasome proteolytic function, as its absence led to the inhibition of BRCA1, FANCD2, and RAD51 foci formation (Figs. 2*D* and 5) but minimally affected FANCD2 monoubiquitination and the proteolytic function of the proteasome (Fig. 2*B*). The role of USP14 in DNA damage–induced foci formation is currently under investigation.

Taken together, our results show for the first time that proteasome function is required for efficient signaling of DNA

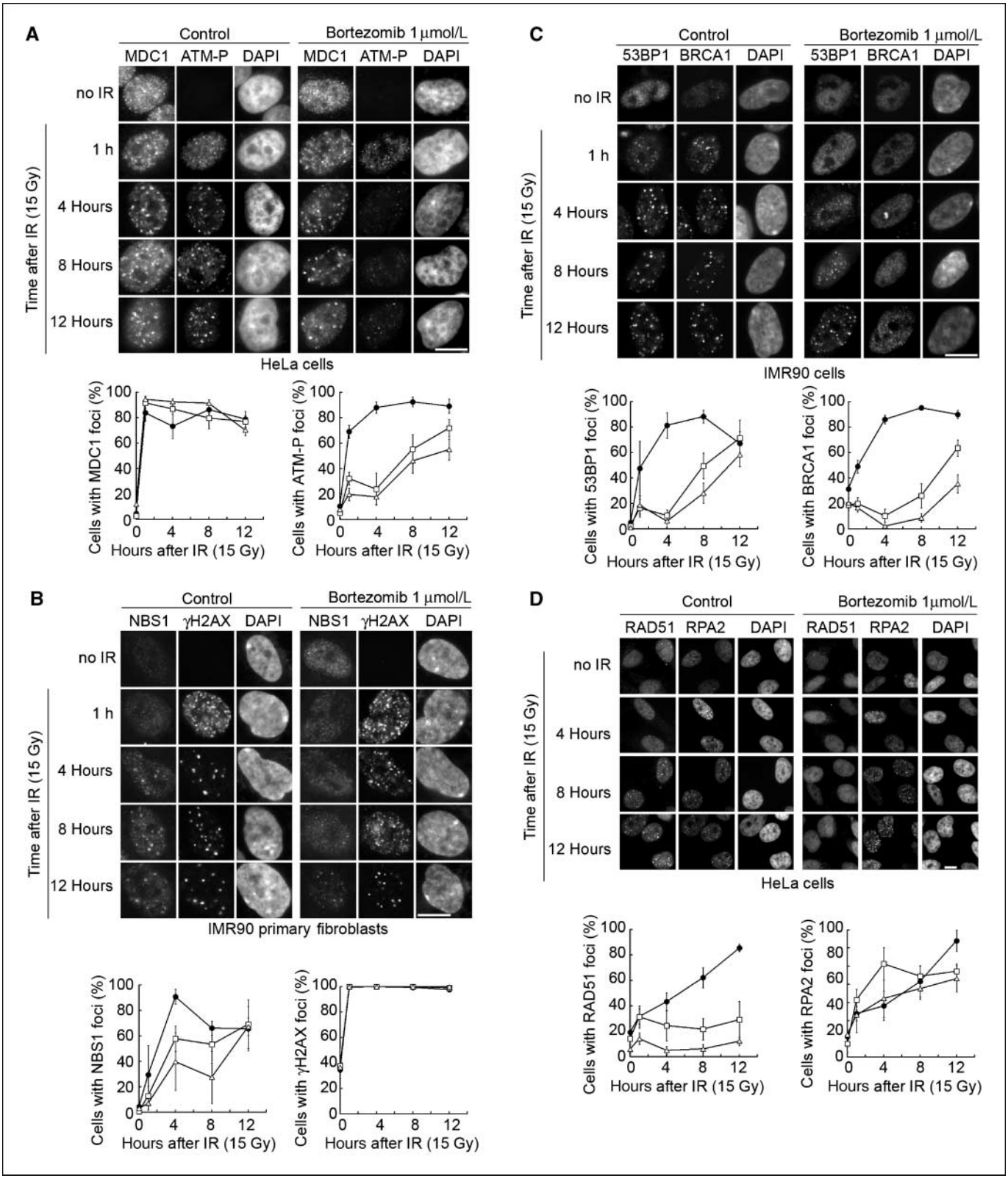

Figure 4. Proteasome inhibitors inhibit IR-induced foci formation of DNA repair proteins. *A,* proteasome inhibition delayed IR-induced phospho-ATM (Ser^{1981}) foci formation without affecting MDC1 foci formation. HeLa cells were pretreated with MG132 (2 μmol/L) or bortezomib (1 μmol/L) for 4 h, irradiated (15 Gy), and incubated for the indicated amount of time. Representative photographs of immunostained cells. Proportion of cells with at least five indicated foci as a function of time after IR in mock-treated (●), MG132-treated (□), or bortezomib-treated (Δ) populations. *Points,* mean; *bars,* SE. *Bar,* 20 μm. *B,* proteasome inhibition mildly delayed IR-induced NBS1 foci formation without disturbing γH2AX foci formation. Cells were treated as indicated in (*A*). *Bar,* 20 μm. *C,* proteasome inhibition strongly delayed IR-induced 53BP1 and BRCA1 foci formation. Cells were treated as indicated in (*A*). *Bar,* 20 μm. *D,* proteasome inhibition inhibited IR-induced RAD51 foci formation without disturbing RPA2 foci formation. Cells were treated as indicated in (*A*). *Bar,* 20 μm.

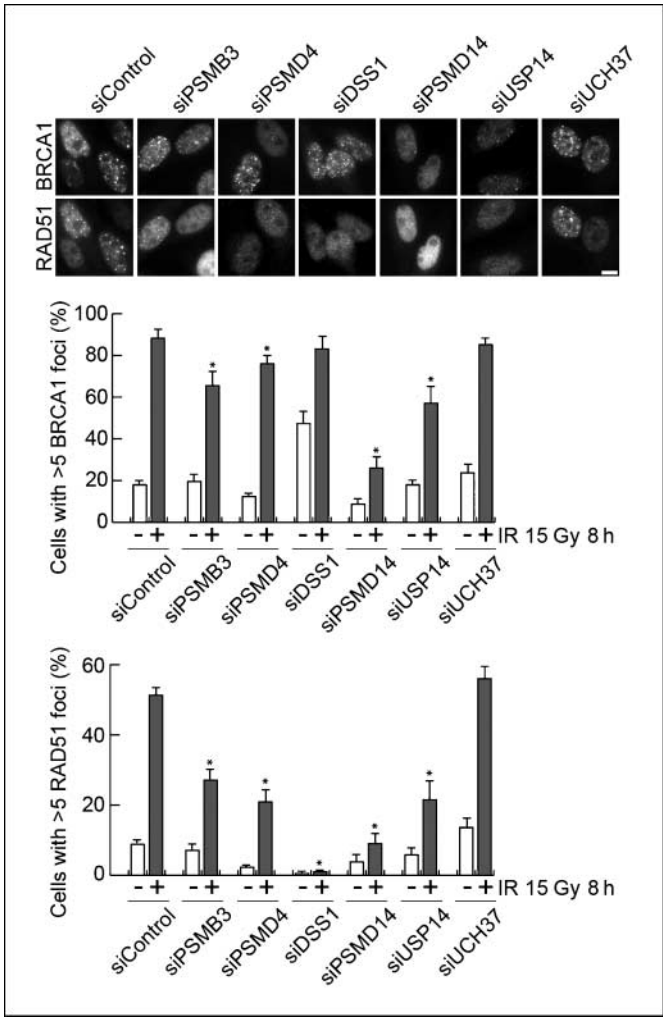

Figure 5. Depletion of PSMB3, PSMD4, PSMD14, and USP14 inhibits IR-induced foci formation of BRCA1 and RAD51, whereas depletion of DSS1 inhibits only RAD51 foci formation. Forty hours after siRNA transfection, HeLa cells were irradiated (15 Gy) and fixed 8 h after IR. Cells were double stained with anti-BRCA1 and anti-RAD51 antibodies. Representative pictures of immunostained cells are shown together with quantification of the cells with at least five BRCA1 or RAD51 foci before (−; *white columns*) and 8 h after IR (+; *gray columns*). *Columns,* mean of four independent experiments; *bars,* SE. *, significant difference with irradiated control siRNA–transfected cells ($P < 0.05$, unpaired *t* test). *Bar,* 20 μm.

damage and recruitment of phospho-ATM, 53BP1, NBS1, BRCA1, FANCD2, and RAD51 at sites of DNA damage.

Inhibition of DNA repair and cell cycle checkpoint activation by proteasome inhibition. Proteasome inhibitors did not inhibit histone H2AX phosphorylation and γH2AX foci formation after DNA damage (Figs. 1*A* and *C* and 4*B*). Instead, we observed that the level of DNA damage–induced H2AX phosphorylation and the number of γH2AX foci per cell remained significantly higher over time in proteasome inhibitor–treated cells compared with mock-treated cells (Figs. 1*C*, 4*B*, and 6*A*), suggesting that DNA repair is impaired in proteasome inhibitor–treated cells, consistently with the impaired recruitment of DNA repair proteins (e.g., RAD51) at sites of DNA damage.

Next, we analyzed the effect of the proteasome inhibitors on cell cycle profile after exposure to IR (Fig. 6*B*). Inhibition of S-phase entry and decrease in the proportion of S-phase cells after IR were observed in MG132-untreated IMR90 primary fibroblasts, indicating that the IR-induced G_1-S checkpoint was activated (37). In contrast, in MG132-treated cells, the proportion of S-phase cells did not decrease after IR, indicating a failure of activation of the G_1-S checkpoint (Fig. 6*B*) despite the accumulation of p53 and p21, regulators of the G_1-S checkpoint, on proteasome inhibition (data not shown). The level of nucleotide incorporation decreased 8 and 12 h after IR exposure in MG132-treated cells (Fig. 6*B*) possibly due to a slower progression of replication due to unrepaired DNA lesions. These results indicate that inhibition of proteasome function alters cell cycle control in the presence of IR-induced DNA damage.

Discussion

DNA-damaging agents (chemotherapeutic drugs and IR) have been used for cancer therapy for decades. The recent emergence of a proteasome inhibitor as anticancer drug rendered its combination with DNA-damaging agents possible in clinical trial and has already given promising results through mechanism(s) yet unknown (9, 10). In this study, we show that proteasome inhibition leads to the inhibition of the general DNA damage response and the Fanconi anemia pathway at multiple levels, leading to the persistence of DNA damage and abrogation of G_1-S cell cycle checkpoint, thus providing for the first time a rationale for the combination therapy.

We found that the proteasome function is required for both basal and DNA damage–induced (IR, UV, DNA cross-linking agents, and hydroxyurea) monoubiquitination of FANCD2, a critical step for the activation of the Fanconi anemia pathway. The mechanisms responsible for the inhibition of FANCD2 monoubiquitination by proteasome inhibition remain unclear, although we ruled out most of the testable possibilities [activation of FANCD2 deubiquitinating enzyme (USP1) and inactivation of the E2 (UBE2T) and E3 (Fanconi anemia core complex) enzymes and the upstream kinase (ATR) required for FANCD2 monoubiquitination] are not responsible for the observed Fanconi anemia pathway inhibition. In addition, although proteasome inhibition leads to the reduction of the free cellular ubiquitin pool (26), the maintenance of PCNA monoubiquitination in response to DNA damage in cells treated with proteasome inhibitors suggests that free ubiquitin is still available to modify nuclear proteins at sites of DNA damage. The fact that FANCD2 monoubiquitination was reduced on short exposure to proteasome inhibitors, even in the absence of USP1, suggested the involvement of another deubiquitinating enzyme yet to be determined. We also found that proteasome inhibition led to the inhibition of recruitment of numerous proteins involved in DNA damage response at site of DNA damage induced by IR and DNA cross-linking agents. Following proteasome inhibition, phospho-ATM, 53BP1, NBS1, and BRCA1 foci formation was delayed, FANCD2 and RAD51 foci were inhibited, whereas γH2AX, MDC1, and RPA foci formed normally, as summarized in Fig. 6*C*.

The MRE11/RAD50/NBS1 complex detects DSBs and triggers the recruitment and activation of ATM kinase through its autophosphorylation on Ser^{1981} (31, 38). Activated ATM phosphorylates numerous substrates, including histone H2AX, NBS1, MDC1, CHK2, SMC1, BRCA1, p53, and FANCD2, activating cell cycle checkpoints, DNA repair, and apoptosis pathways (39). Histone H2AX phosphorylation induces MDC1 recruitment (40). Our findings that foci formation of γH2AX and MDC1 and phosphorylation of ATM substrates (ATM, CHK2, NBS1, and FANCD2) were not affected by

proteasome inhibition indicate that proteasome is not implicated in these early DNA damage–signaling steps.

Foci formation of MDC1, 53BP1, and phospho-ATM occurs rapidly after IR in an interdependent manner. 53BP1 recruitment is dependent on MDC1, ATM (41), methylation of histone H4 Lys^{20} (42), and increased exposure of histone H3 methyl Lys^{79} due to DSB-induced chromatin relaxation (43). Phospho-ATM recruitment is dependent on MDC1 (44) and 53BP1 (data not shown). We showed that both 53BP1 and phospho-ATM foci were inhibited on proteasome inhibition, whereas MDC1 foci formation and ATM

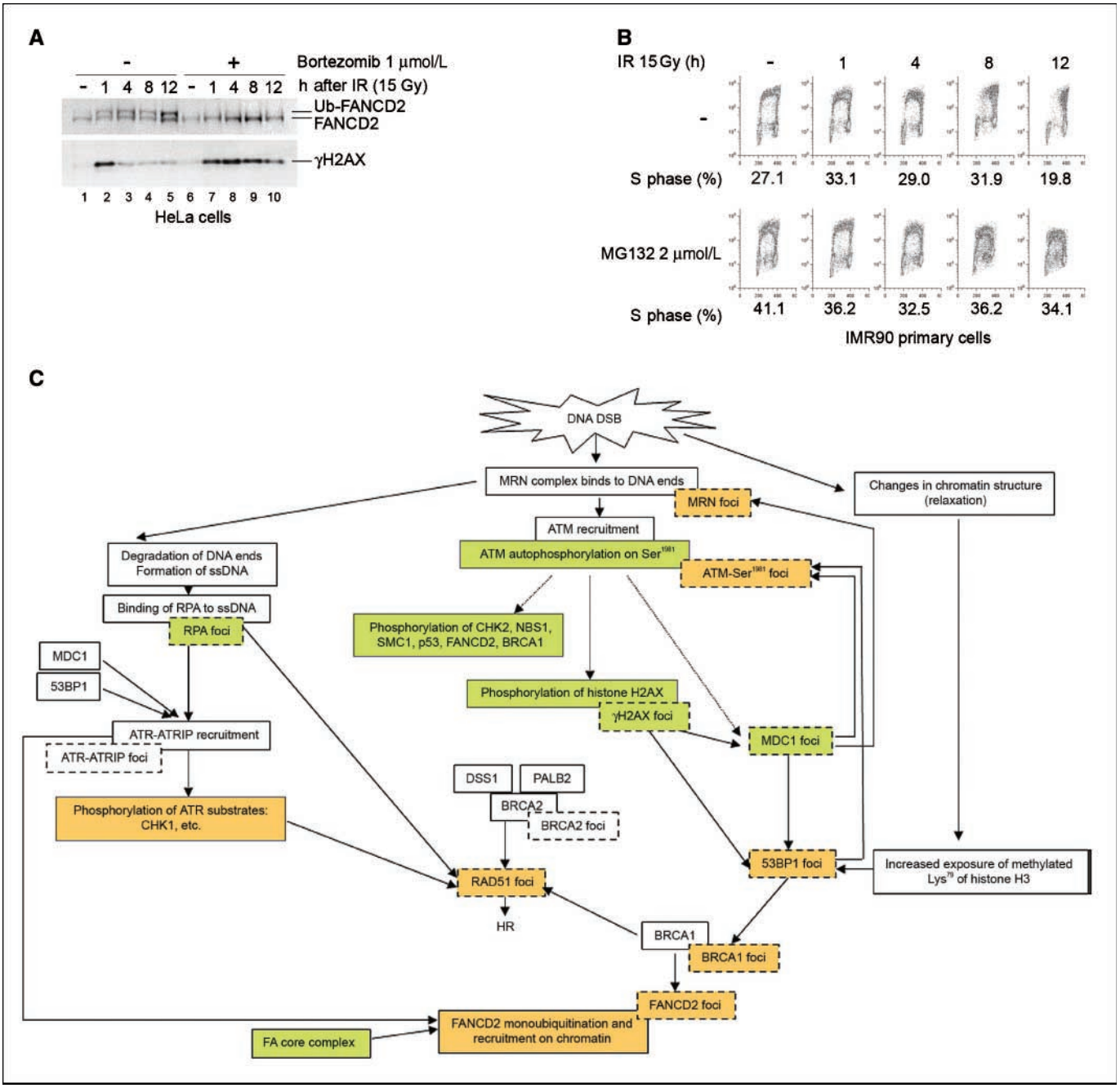

Figure 6. Proteasome inhibition inhibits DNA repair and cell cycle checkpoint. (Full-length blots are presented in Supplementary Fig. S3*K*). *A,* proteasome inhibition led to persistent histone H2AX phosphorylation after DNA damage. HeLa cells were pretreated with bortezomib (1 μmol/L) for 4 h, irradiated (15 Gy), and incubated for the indicated amount of time after IR. Whole-cells extracts were used for detection of FANCD2 and histone H2AX phosphorylation on Ser^{139} (*γH2AX*). *B,* proteasome inhibition impaired IR-induced cell cycle checkpoints. IMR90 primary fibroblasts were pretreated in MG132 (2 μmol/L) for 4 h, irradiated (15 Gy), and incubated for the indicated amount of time after IR. Fifteen minutes before fixation, cells were pulse labeled with BrdUrd (30 μmol/L). Incorporation of BrdUrd (*Y axis*) and DNA content (propidium iodide; *X axis*) was quantified by flow cytometry. Representative flow cytometric analyses and the mean value of the proportion of cells in S phase are shown for each condition. *C,* schematic representation of the cellular response to IR-induced DNA damage. *Orange,* events sensitive to proteasome inhibition; *light green,* events resistant to proteasome inhibition. Proteasome inhibition–sensitive events include monoubiquitination of FANCD2, foci formation of 53BP1, phospho-ATM, NBS1, BRCA1, FANCD2, and RAD51, and IR-induced phosphorylation of CHK1. Proteasome inhibition–resistant events include ATM autophosphorylation (Ser^{1981}), phosphorylation of H2AX (Ser^{139}), CHK2 (Thr^{68}), NBS1 (Ser^{343}), and FANCD2 (Thr^{691}), and nuclear foci formation of γH2AX, MDC1, and RPA (see Discussion for the detail). *DNA DSB*, DNA double-strand break. *FA,* Fanconi anemia. *HR*, homologous recombination.

autophosphorylation remained unaffected, as well as histone H4 Lys^{20} methylation (data not shown). Induction of chromatin relaxation using hypotonic buffer, histone deacetylase inhibitors (trichostatin A and sodium butyrate), or chloroquine did not restore 53BP1 foci formation (data not shown), suggesting that inhibition of 53BP1 foci formation is not simply due to abnormally condensed chromatin on proteasome inhibition. Thus, our results suggest that proteasome proteolytic function is required for recruitment of 53BP1 at sites of DNA damage marked by H2AX phosphorylation and MDC1 recruitment. Lack of phospho-ATM foci may in turn be subsequent to inhibition of 53BP1 foci.

BRCA1 and MRN complex foci form after MDC1/53BP1/phospho-ATM foci. BRCA1 foci formation depends on MDC1 (40, 44) and 53BP1 (45), whereas accumulation of the MRN complex in nuclear foci depends at least on MDC1 (44). We showed that BRCA1 and NBS1 foci formation was delayed on proteasome inhibition, which, in the case of BRCA1, may be a consequence of proteasome inhibition–induced inhibition of 53BP1 foci.

Proteasome inhibition–induced inhibition of FANCD2 monoubiquitination may explain inhibition of FANCD2 foci formation. However, FANCD2 foci formation was more severely affected than FANCD2 monoubiquitination in cells depleted for proteasome subunits, suggesting that inhibition of FANCD2 monoubiquitination requires a more profound proteasome inhibition than inhibition of foci formation. For example, in PSMD4- or PSMB3-depleted cells, FANCD2 monoubiquitination was minimally inhibited (Fig. 2*C*) but its foci formation was clearly inhibited (Fig. 2*D*), suggesting that the proteasome function is required for accumulation of monoubiquitinated FANCD2 in nuclear foci. The inhibition of FANCD2 foci formation by the proteasome inhibition may be secondary to impaired BRCA1 foci formation, as FANCD2 foci formation is dependent on BRCA1 (12).

RAD51 foci formation depends on formation of ssDNA (46). The RPA complex binds ssDNA and allows the recruitment of ATR-ATRIP complex, RAD17, and RAD9. RAD51 displaces RPA from ssDNA and catalyzes strand invasion required for homology-directed repair (46). CHK1 kinase activity, BRCA1, and BRCA2 are required for RAD51 recruitment (47–49). We observed that RAD51 foci formation was inhibited on proteasome inhibition, whereas RPA foci were not affected, suggesting that the generation of ssDNA, required for RAD51 binding and HR, is not altered by proteasome inhibition. BRCA1 foci and IR-induced CHK1 phosphorylation were inhibited on proteasome inhibition, which may lead to lack of RAD51 foci. The observed delay/inhibition of DNA repair, revealed by the persistence of histone H2AX phosphorylation, may be due to the proteasome inhibition–induced inhibition of RAD51 foci formation, which will cause defect of HR. FANCD2 and RAD51 foci formation in response to DNA damage has recently been shown to depend on HCLK2 (50). Whether HCLK2 is affected by proteasome inhibition remains to be determined.

Taken together, our results reveal a new role of proteasome proteolytic function in maintaining yet unidentified steps downstream of MDC1 and RPA foci formation, which control the foci formation of 53BP1, phospho-ATM, BRCA1, NBS1, FANCD2, and RAD51. The identification of these proteasome targets required for the formation of these foci is ongoing.

As studies in budding yeast showed that subunits of both 19S and 20S proteasomes are recruited to the site of DSB (18), it is tempting to speculate that in human cells also the proteasome accumulates at sites of DSB and is required for the recruitment of DNA damage response/repair proteins. In that case, our results suggest that the role of the proteasome at DSB would be to degrade one or more proteins present at site of DNA damage during DNA damage signaling rather than following the completion of DNA repair. However, we were unable to reproducibly detect DNA damage–inducible nuclear foci of the proteasome using six different antibodies against different subunits of the proteasome (data not shown). Whether the proteasome accumulates at sites of DNA damage in mammalian cells remains unclear.

In summary, we conclude that the proteasome is involved in many aspects of DNA damage response and controls monoubiquitination of FANCD2, foci formation of 53BP1, phospho-ATM, NBS1, BRCA1, FANCD2, and RAD51, and IR-induced activation of ATR-CHK1. Proteasome inhibitors may sensitize tumor cells to DNA-damaging agents through the inhibition of these processes.

Acknowledgments

Received 3/19/2007; revised 5/18/2007; accepted 5/24/2007.

Grant support: Searle Scholars Program and Mary Kay Ash Charitable Foundation Cancer Research Project Grant (T. Taniguchi) and Fondation Bettencourt Schueller (C. Jacquemont).

The costs of publication of this article were defrayed in part by the payment of page charges. This article must therefore be hereby marked *advertisement* in accordance with 18 U.S.C. Section 1734 solely to indicate this fact.

We thank Drs. Alan D'Andrea, Tony Huang, C. Grandori, R. Meetei, T.R. Singh, S. Takeda, and W. Sakai for helpful discussion and critical reading of the manuscript; E. Villegas for technical assistance; M. Hogan for irradiating our cells; and Drs. Tony Huang, Alan D'Andrea, X. Wang, M. Hoatlin, W. Wang, Junjie Chen, and Muneesh Tewari for reagents.

References

1. Pickart CM, Cohen RE. Proteasomes and their kin: proteases in the machine age. Nat Rev Mol Cell Biol 2004;5:177–87.
2. Sigismund S, Polo S, Di Fiore PP. Signaling through monoubiquitination. Curr Top Microbiol Immunol 2004; 286:149–85.
3. Berkers CR, Verdoes M, Lichtman E, et al. Activity probe for *in vivo* profiling of the specificity of proteasome inhibitor bortezomib. Nat Methods 2005;2: 357–62.
4. Adams J. The proteasome: a suitable antineoplastic target. Nat Rev Cancer 2004;4:349–60.
5. Caravita T, de Fabritiis P, Palumbo A, Amadori S, Boccadoro M. Bortezomib: efficacy comparisons in solid tumors and hematologic malignancies. Nat Clin Pract Oncol 2006;3:374–87.
6. Pajonk F, Pajonk K, McBride WH. Apoptosis and radiosensitization of hodgkin cells by proteasome inhibition. Int J Radiat Oncol Biol Phys 2000;47:1025–32.
7. Mitsiades N, Mitsiades CS, Richardson PG, et al. The proteasome inhibitor PS-341 potentiates sensitivity of multiple myeloma cells to conventional chemotherapeutic agents: therapeutic applications. Blood 2003;101: 2377–80.
8. Yunmbam MK, Li QQ, Mimnaugh EG, et al. Effect of the proteasome inhibitor ALLnL on cisplatin sensitivity in human ovarian tumor cells. Int J Oncol 2001;19:741–8.
9. Berenson JR, Yang HH, Sadler K, et al. Phase I/II trial assessing bortezomib and melphalan combination therapy for the treatment of patients with relapsed or refractory multiple myeloma. J Clin Oncol 2006;24: 937–44.
10. Aghajanian C, Dizon DS, Sabbatini P, Raizer JJ, Dupont J, Spriggs DR. Phase I trial of bortezomib and carboplatin in recurrent ovarian or primary peritoneal cancer. J Clin Oncol 2005;23:5943–9.
11. Taniguchi T, D'Andrea AD. Molecular pathogenesis of Fanconi anemia: recent progress. Blood 2006;107: 4223–33.
12. Garcia-Higuera I, Taniguchi T, Ganesan S, et al. Interaction of the Fanconi anemia proteins and BRCA1 in a common pathway. Mol Cell 2001;7:249–62.
13. Taniguchi T, Garcia-Higuera I, Andreassen PR, Gregory RC, Grompe M, D'Andrea AD. S-phase-specific interaction of the Fanconi anemia protein, FANCD2, with BRCA1 and RAD51. Blood 2002;100:2414–20.
14. Andreassen PR, D'Andrea AD, Taniguchi T. ATR couples FANCD2 monoubiquitination to the DNA-damage response. Genes Dev 2004;18:1958–63.
15. Meetei AR, de Winter JP, Medhurst AL, et al. A novel ubiquitin ligase is deficient in Fanconi anemia. Nat Genet 2003;35:165–70.

16. Machida YJ, Machida Y, Chen Y, et al. UBE2T is the E2 in the Fanconi anemia pathway and undergoes negative autoregulation. Mol Cell 2006;23:589–96.
17. Nijman SM, Huang TT, Dirac AM, et al. The deubiquitinating enzyme USP1 regulates the Fanconi anemia pathway. Mol Cell 2005;17:331–9.
18. Krogan NJ, Lam MH, Fillingham J, et al. Proteasome involvement in the repair of DNA double-strand breaks. Mol Cell 2004;16:1027–34.
19. Marston NJ, Richards WJ, Hughes D, Bertwistle D, Marshall CJ, Ashworth A. Interaction between the product of the breast cancer susceptibility gene BRCA2 and DSS1, a protein functionally conserved from yeast to mammals. Mol Cell Biol 1999;19:4633–42.
20. Li J, Zou C, Bai Y, Wazer DE, Band V, Gao Q. DSS1 is required for the stability of BRCA2. Oncogene 2006;25:1186–94.
21. Gudmundsdottir K, Lord CJ, Witt E, Tutt AN, Ashworth A. DSS1 is required for RAD51 focus formation and genomic stability in mammalian cells. EMBO Rep 2004;5:989–93.
22. Taniguchi T, Tischkowitz M, Ameziane N, et al. Disruption of the Fanconi anemia-BRCA pathway in cisplatin-sensitive ovarian tumors. Nat Med 2003;9:568–74.
23. Bence NF, Sampat RM, Kopito RR. Impairment of the ubiquitin-proteasome system by protein aggregation. Science 2001;292:1552–5.
24. Huang TT, Nijman SM, Mirchandani KD, et al. Regulation of monoubiquitinated PCNA by DUB autocleavage. Nat Cell Biol 2006;8:339–47.
25. Huang TT, D'Andrea AD. Regulation of DNA repair by ubiquitylation. Nat Rev Mol Cell Biol 2006;7:323–34.
26. Dantuma NP, Groothuis TA, Salomons FA, Neefjes J. A dynamic ubiquitin equilibrium couples proteasomal activity to chromatin remodeling. J Cell Biol 2006;173:19–26.
27. Borodovsky A, Kessler BM, Casagrande R, Overkleeft HS, Wilkinson KD, Ploegh HL. A novel active site-directed probe specific for deubiquitylating enzymes reveals proteasome association of USP14. EMBO J 2001;20:5187–96.
28. Reuter TY, Medhurst AL, Waisfisz Q, et al. Yeast two-hybrid screens imply involvement of Fanconi anemia proteins in transcription regulation, cell signaling, oxidative metabolism, and cellular transport. Exp Cell Res 2003;289:211–21.
29. Heinrich MC, Silvey KV, Stone S, et al. Posttranscriptional cell cycle-dependent regulation of human FANCC expression. Blood 2000;95:3970–7.
30. Liu Q, Guntuku S, Cui XS, et al. Chk1 is an essential kinase that is regulated by Atr and required for the G(2)/M DNA damage checkpoint. Genes Dev 2000;14:1448–59.
31. Bakkenist CJ, Kastan MB. DNA damage activates ATM through intermolecular autophosphorylation and dimer dissociation. Nature 2003;421:499–506.
32. Lim DS, Kim ST, Xu B, et al. ATM phosphorylates p95/nbs1 in an S-phase checkpoint pathway. Nature 2000;404:613–7.
33. Matsuoka S, Rotman G, Ogawa A, Shiloh Y, Tamai K, Elledge SJ. Ataxia telangiectasia-mutated phosphorylates Chk2 *in vivo* and *in vitro*. Proc Natl Acad Sci U S A 2000;97:10389–94.
34. Ho GP, Margossian S, Taniguchi T, D'Andrea AD. Phosphorylation of FANCD2 on two novel sites is required for mitomycin C resistance. Mol Cell Biol 2006;26:7005–15.
35. Binz SK, Sheehan AM, Wold MS. Replication protein A phosphorylation and the cellular response to DNA damage. DNA Repair (Amst) 2004;3:1015–24.
36. Josse L, Harley ME, Pires IM, Hughes DA. Fission yeast Dss1 associates with the proteasome and is required for efficient ubiquitin-dependent proteolysis. Biochem J 2006;393:303–9.
37. Xu B, Kastan MB. Analyzing cell cycle checkpoints after ionizing radiation. Methods Mol Biol 2004;281:283–92.
38. Lee JH, Paull TT. ATM activation by DNA double-strand breaks through the Mre11-Rad50-Nbs1 complex. Science 2005;308:551–4.
39. Shiloh Y. ATM and related protein kinases: safeguarding genome integrity. Nat Rev Cancer 2003;3:155–68.
40. Stucki M, Clapperton JA, Mohammad D, Yaffe MB, Smerdon SJ, Jackson SP. MDC1 directly binds phosphorylated histone H2AX to regulate cellular responses to DNA double-strand breaks. Cell 2005;123:1213–26.
41. Bekker-Jensen S, Lukas C, Melander F, Bartek J, Lukas J. Dynamic assembly and sustained retention of 53BP1 at the sites of DNA damage are controlled by Mdc1/NFBD1. J Cell Biol 2005;170:201–11.
42. Botuyan MV, Lee J, Ward IM, et al. Structural basis for the methylation state-specific recognition of histone H4-K20 by 53BP1 and Crb2 in DNA repair. Cell 2006;127:1361–73.
43. Huyen Y, Zgheib O, Ditullio RA, Jr., et al. Methylated lysine 79 of histone H3 targets 53BP1 to DNA double-strand breaks. Nature 2004;432:406–11.
44. Lou Z, Minter-Dykhouse K, Franco S, et al. MDC1 maintains genomic stability by participating in the amplification of ATM-dependent DNA damage signals. Mol Cell 2006;21:187–200.
45. Wang B, Matsuoka S, Carpenter PB, Elledge SJ. 53BP1, a mediator of the DNA damage checkpoint. Science 2002;298:1435–8.
46. Wang X, Haber JE. Role of saccharomyces single-stranded DNA-binding protein RPA in the strand invasion step of double-strand break repair. PLoS Biol 2004;2:E21.
47. Sorensen CS, Hansen LT, Dziegielewski J, et al. The cell-cycle checkpoint kinase Chk1 is required for mammalian homologous recombination repair. Nat Cell Biol 2005;7:195–201.
48. Bhattacharyya A, Ear US, Koller BH, Weichselbaum RR, Bishop DK. The breast cancer susceptibility gene BRCA1 is required for subnuclear assembly of Rad51 and survival following treatment with the DNA cross-linking agent cisplatin. J Biol Chem 2000;275:23899–903.
49. Davies AA, Masson JY, McIlwraith MJ, et al. Role of BRCA2 in control of the RAD51 recombination and DNA repair protein. Mol Cell 2001;7:273–82.
50. Collis SJ, Barber LJ, Clark AJ, Martin JS, Ward JD, Boulton SJ. HCLK2 is essential for the mammalian S-phase checkpoint and impacts on Chk1 stability. Nat Cell Biol 2007;9:391–401.